Eur. Phys. J. E (2018) **41**: 26
DOI 10.1140/epje/i2018-11632-9

THE EUROPEAN PHYSICAL JOURNAL E

Regular Article

Influence of the static field on a heavy body in a rotating drum with liquid*

Olga Vlasova[1,a] and Nikolai Kozlov[2,b]

[1] Laboratory of Vibrational Hydromechanics, Perm State Humanitarian Pedagogical University – 24, Sibirskaya, 614990, Perm, Russia
[2] Laboratory of Hydrodynamic Stability, Institute of Continuous Media Mechanics UrB RAS, PFRC – 1, Akademika Koroleva, 614013, Perm, Russia

Received 15 August 2017 and Received in final form 6 December 2017
Published online: 20 February 2018 –

Abstract. The behaviour of a heavy cylindrical body in a rotating horizontal cylindrical cavity filled with viscous liquid is investigated experimentally. Several modes of the body behaviour depending on the rate of the cavity rotation, *i.e.*, the ratio of the centrifugal force of inertia and the gravity, are detected. At a fast rotation rate, the body makes the solid-body rotation, remaining immobile relative to the cavity due to the action of the centrifugal force. In the absence of rotation, under the influence of gravity, the body occupies a position in the lower part of the cavity. At slow uniform rotation rate, the body is dragged by the cavity boundary and shifts to some angle relative to the initial position. With an increase in the rotation rate, the body is repulsed from the cavity boundary and occupies a suspended position, stationary in the laboratory frame, at a certain distance from it. In the suspension regime and the partial repulsion regime, which precedes it, the body performs auto-oscillations that resemble the precession. The flow structures near the suspended cylinder are studied using the PIV method.

Introduction

The dynamics of multiphase systems refers to numerous situations encountered in nature and technology. Among others, there are density-inhomogeneous hydrodynamic systems, which are susceptible to the influence by inertial fields. A particular case is when the inertia force acting on these systems arises due to the action of vibrations or rotation. Problems on equilibrium and stability are crucial for density-inhomogeneous multiphase systems in oscillating inertia fields.

As is known, the oscillating motion of inhomogeneous hydrodynamic systems leads to the appearance of averaged effects. This class of problems is of particular interest under zero-gravity conditions, since the oscillatory effect on such a system can lead to the appearance of averaged forces that act on inclusions near the solid boundary. Inclusions can be of various shapes and densities, gaseous and solid. In studies [1–3] it is revealed that in a viscous fluid the averaged lift force acts on a vibrating body near the cavity boundary. As a result, the body repels from the wall. The lift force occurs as a result of an asymmetric distribution of the average pressure over the surface of the oscillating body and appears at a distance comparable to the thickness of the Stokes boundary layer.

The dynamics of density-inhomogeneous hydrodynamic systems at rotation is of great interest [4]. The control of inclusions of various types in these systems is an actual problem caused by a large number of practical applications. A special case for this class of problems is the dynamics of a solid body in a rotating cavity with liquid. Depending on the density and rotation speed, the body can occupy a stable position near the wall or near the axis of rotation. In [5], a situation of two rotating cylinders in a viscous fluid was considered and it was shown that the torques acting on the cylinders are determined by their relative position and size and by their rotation rates. In [6], the dynamics of the cylindrical body in a low-viscosity liquid in a rotating drum is studied. It is found that at a low rotation rate of the drum the body rolls on the rotating wall. At the critical rotation rate, the body repels from the wall and gets into the suspended state. In both states the body rotates around its axis: in the first state, its rotation occurs in the direction of the drum rotation, in the second one, in the opposite direction. In [7] the rolling down of a very heavy cylinder along the wall of a rotating horizontal cylindrical cavity with a high-viscosity liquid is studied. The cylinder is carried away by the rotating cavity wall

* Contribution to the Topical Issue "Non-equilibrium processes in multicomponent and multiphase media" edited by Tatyana Lyubimova, Valentina Shevtsova, Fabrizio Croccolo.

[a] e-mail: vlasova_oa@pspu.ru
[b] e-mail: kozlov.n@icmm.ru

and, rising at some angle, slides along the boundary simultaneously rotating around its axis. At fast rotation of the cavity, a chain of cavitation bubbles is formed between the body and the wall, and the body is counter-rotating with respect to the cavity.

The study of the flow structure near the phase inclusions in the considered systems is of great scientific interest. It is due to the fact that the presence of some inclusion in a rotating liquid leads to a transformation of the flow. This process depends on the dimensions and the shape of the inclusion: it may cause an intensification of the mass transfer or bring to some negative effects. In [7, 8] the flow structure near the inclusion is analyzed using the PIV (Particle Image Velocimetry) method. In the case of a small air bubble, the flow disturbance is rapidly damped [8]; in the case of a cylinder, in [7], they observed a change in the velocity profile of the fluid motion and a significant decrease of its value. The dynamics of the body also influences the flow structure. It is known that if the infinite fluid flows around a body at rest, the form of the wake behind the body is determined by the Reynolds number [9]: $\mathrm{Re} \equiv V_f 2r/\nu$, where V_f is the velocity of the incoming flow, $2r$ is the body diameter, ν is the kinematic viscosity of the fluid. At the value $\mathrm{Re} \sim 10^2$ the vortex pair is formed behind the immobile cylinder. The rotation of the cylinder produces an asymmetry of the flow around it [10,11]: behind the body only one vortex is observed, displaced relative to its axis in the direction of its rotation. The presence of the solid boundary near the body also leads to the transformation of the flow around the body [9].

The purpose of our research is to study the influence of a static field (gravity) on the behaviour of a heavy cylindrical body in a horizontal uniformly rotating cavity with liquid. The dynamics of the cylinder is investigated depending on the cavity rotation rate. The first experimental results were published in [12]. The present work extends this research with more profound experimental data, especially, on the flow structures near the cylinder, which are studied using the Particle Image Velocimetry (PIV) technique.

Experimental method and results

The experimental investigation of a cylindrical body behaviour in the rotating container filled with liquid is conducted. The cuvette 1 has a cylindrical cavity of radius $R = 30.0\,\mathrm{mm}$ and length $L = 74.0\,\mathrm{mm}$. It is made of transparent acrylic glass with wall thickness 4.0 mm (fig. 1). In experiments, the aluminium cylindrical body 2 is used. It has a radius $r = 4.7\,\mathrm{mm}$, a length $l = 60.0\,\mathrm{mm}$ and density $\rho_S = 3.04\,\mathrm{g/cm^3}$. On the ends of the body, markers are fixed, which allow to track its rotation around its own axis.

The cavity with the cylinder inside it is filled with an aqueous solution of glycerine with viscosity $\nu = 0.59\,\mathrm{St}$ and density $\rho_L = 1.21\,\mathrm{gr/cm^3}$. The viscosity of the working fluid is measured with a capillary viscometer of the type VPZh-2, the relative error does not exceed 1%. The

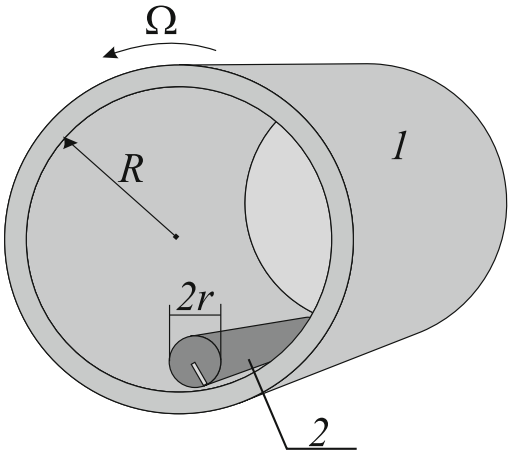

Fig. 1. The container with a cylinder placed in it.

density is measured with a hydrometer, the accuracy is $0.01\,\mathrm{g/cm^3}$. The temperature of the air in the laboratory is kept at about 24 °C (the deviation does not exceed 1 degree). The body used in the experiments is considered "heavy", since its density exceeds the density of the liquid. The relative density of the body is $\rho \equiv \rho_S/\rho_L = 2.51$. The filled cuvette is fixed to the shaft 3, which is installed in the support 4 (fig. 2). Through the coupling 5, a stepper motor 6 of the type Electroprivod FL86STH118-6004A transmits rotation with angular velocity Ω to the cavity. The rotation rate is controlled with a DAC ZetLab Zet-410 and varies in the range from 1 to 30 rad/s (accuracy of measurement 0.06 rad/s). The installation is rigidly fixed to the platform 7. A high-speed video camera 8 Optronis CamRecord CL600x2 is used for video registration at illumination of the cavity by a powerful light source.

The dynamics of the body is monitored through the front end of the cavity (fig. 3). The video camera is placed at a distance of 40–50 cm from the cavity front end. The coaxial position of the camera and the cuvette is ensured by the method of combining the marks indicating the centres of the anterior and posterior ends of the cavity. The frame frequency is 500 frames per second at a resolution of 800×800 pixels per frame. In the photographs and diagrams below, the cavity rotates counter-clockwise. The video recordings captured in the experiments are divided into frames and processed using a computer. When measuring the azimuthal position of the body ϕ_b in the laboratory reference frame, the position at the lowest point of the cavity is taken as the zero value, the direction of the counter-clockwise passage is considered positive.

At rest, the cylinder, whose density is greater than that of the liquid, is at the bottom of the cavity. The cavity is brought into slow rotation, and the body is dragged by the cavity wall due to the frictional force and shifts to some angle ϕ_b. The rotation rate Ω is increased step by step, and at each step, a video registration of the body behaviour is performed. Experimental videos are divided into frames and processed on the computer. In each series of photographs, the azimuthal and radial coordinates of the body are measured as a function of time; in addition,

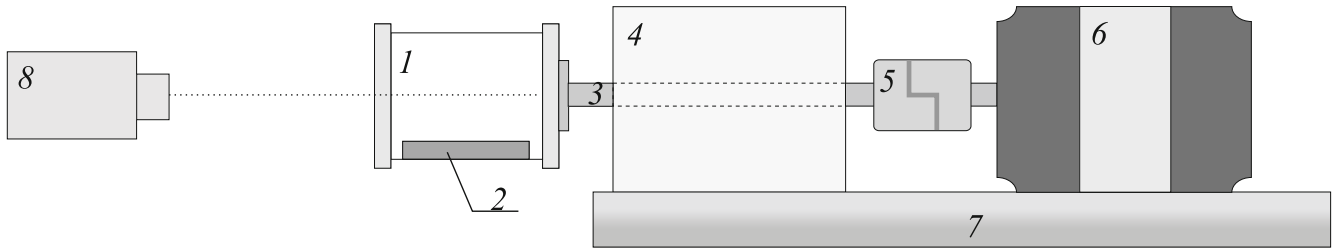

Fig. 2. Scheme of the experimental setup (side view).

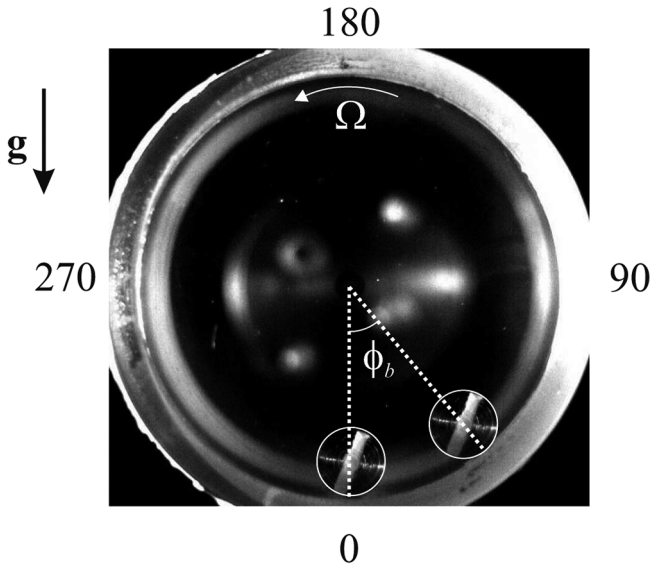

Fig. 3. The front view of the cavity and the measurement scheme of the angle ϕ_b.

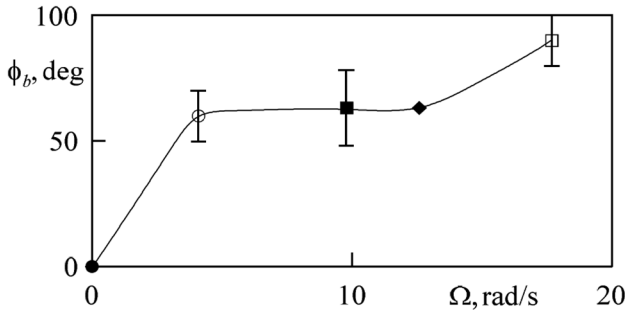

Fig. 4. Variation of the average azimuthal coordinate of the body ϕ_b with Ω.

the position of the marker on the front end of the cylinder is measured. The azimuthal angle ϕ_b is measured in the direction of the cavity rotation. The gap between the cylinder and the cavity wall is measured along the radius of the cavity from the wall towards the centre, $d = R - (R_b + r)$. Here, R_b is the distance between the cavity centre and the centre of the cylinder. This method allows to measure the gap between the body and the cavity wall with an error not exceeding 0.1 mm.

When studying the behaviour of the heavy body in the horizontal rotating cylinder with liquid, the body motion regimes are detected, which are qualitatively different from each other depending on the cavity rotation rate. The time dynamics is investigated and the trajectories of the body motion are constructed for various Ω. Depending on the rotation rate it is possible to identify some characteristic conditions of the body, alternating with a smooth increase in Ω (fig. 4):

◯ slip along the cavity boundary;
■ "walking" cylinder;
♦ stationary body suspension;
□ instability of the suspended state;
transition of the body in the centrifuged state.

All these states are determined by the ratio between the centrifugal force and the gravity force, this is, by the parameter $\Gamma \equiv g/\Omega^2 R$. When $\Gamma < 1$, the system is in the centrifuged state, and the body moves with the fluid as a whole. On the graph, a solid circle marks the initial position of the body in the lower part of the cavity ($\Omega = 0$), the symbols show the average position of the body, the intervals mark the maximum deviation from the average position. With the gradual increase in Ω, the body, due to the viscous interaction, is dragged by the moving wall of the cavity. Its azimuthal coordinate is increasing with Ω. This happens until a certain critical value of ϕ_b, then the mean azimuthal position of the body almost does not change with increasing Ω. With a further increase in Ω, after the transition of the body into the suspended state, it rises up along the azimuthal coordinate up to the value $\phi_b \approx 90°$. Meanwhile, the body maintains its stable position at some distance from the cavity wall. At $\phi_b \approx 90°$ the stationary suspended state of the body loses its stability and it begins to swing, making oscillations resembling precession. An increase in the cavity rotation rate leads to an increase in the amplitude of the body oscillations, while the average azimuthal position of the body remains unchanged. Under the conditions of this experiment, upon reaching the value $\Omega = 22\,\mathrm{rad/s}$ ($\Gamma = 0.68$) the "capture" of the body takes place. It is carried away by the liquid rotating with the cavity and makes practically a solid-state rotation with the cavity and the liquid.

"Sliding" along the cavity boundary. When the cuvette is at rest, the body under the action of gravity is located at the lower boundary of the cavity (fig. 3). With a smooth increase in the rotation rate Ω, the cylinder is displaced along with the wall. After reaching the critical value of the angle (for a given rotation speed) the body rolls (or slides on a very thin fluid layer) along the cavity bound-

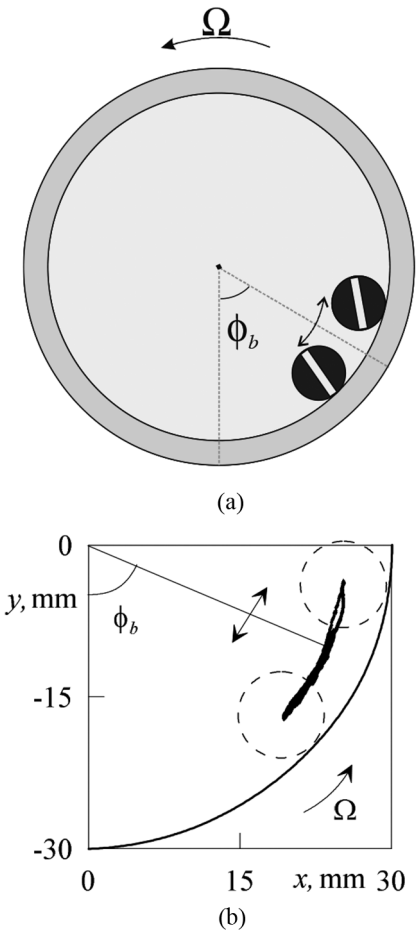

Fig. 5. Scheme of characteristic positions of the cylinder in the rotating cavity (a). Trajectory of motion of the body centre (b).

ary downwards. Then, it rises again without reaching the bottom of the cavity. Thus, the body performs periodic motion up and down along the cavity wall (fig. 5).

Figure 5(a) shows extreme body positions and marks the average value of the angle ϕ_b, about which the body oscillates. At the uniform rotation of the cavity, the body moves up and down along the boundary of the cavity (fig. 5(b)). The trajectory of the center of the cylinder front end on the plane x, y is shown by the points, the arrows show the motion direction. Here and later, on the schemes, $y = 0$ stands for the center of the cavity, $y = -30$ mm corresponds to the cavity boundary, the solid line (arc) is the boundary of the cavity. The dashed circle shows the contours of the cylinder front end at the extreme positions. In the conditions of the present experiment at $\Omega = 4.1$ rad/s the body displaces by the angle $\phi_b \approx 60°$ and oscillates about this position with an amplitude of approximately 10°. This angle ϕ_b is critical, and with the further increase in Ω it does not change. The azimuthal oscillations of the cylinder near the cavity boundary can be associated with periodical alternation of the dry friction and the sliding friction whith the variation of the angle ϕ_b.

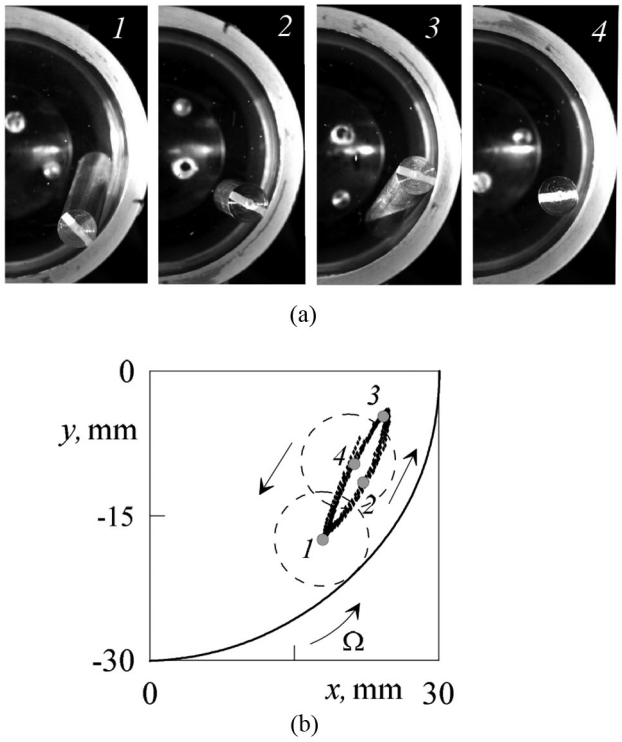

Fig. 6. The position of the body in different phases of "walking" (a). The trajectory of the centre of the cylinder front end in the laboratory frame of reference (b).

In addition to the azimuthal oscillations along the cavity wall, the body rotates around its own axis. The angle of the body rotation α varies irregularly with time. The maximum values of the rotation rate of the body around its own axis are observed during the motion of the body along the walls of the cavity up or down, *i.e.* when the coordinate ϕ_b changes. The rate $\mathrm{d}\alpha/\mathrm{d}t$ reaches the value 17.5 rad/s. At the extreme positions, when the body stops the rotation angle does not change ($\mathrm{d}\alpha/\mathrm{d}t = 0$). The absence of rotation in this case can be associated with a change in the nature of the interaction between the body and the wall.

"Walking" cylinder. With an increase in the speed of the cavity rotation at a critical value of Ω, one of the ends of the cylinder moves away from the cavity boundary, while the second one stays in contact with it. The rotating boundary drags the body end it is in contact with and lifts it in the laboratory frame, while the detached end descends. When the falling end of the body reaches the cavity boundary, it starts moving along with the wall, and the opposite end then moves away from it. Thus, the cylinder "walks" along the moving wall of the cavity, as if it was making large steps alternately leaning on the boundary with one or the other end. Meanwhile the body average position in the laboratory frame does not change with time.

Figure 6 shows the pictures of consecutive body positions during its "walk" (a) and the trajectory of the body front end motion (b) at $\Omega = 9.8$ rad/s. On the plane x, y

the trajectory of the centre of the front end of the cylinder is shown with the points, the arrows indicate the motion direction. The position of the end face of the body during the upward motion is indicated with points 1, 2, 3 and during the downward motion —with points 3, 4, 1.

It is seen that the end face of the body is in contact with the cavity wall while moving upwards and during the descent the end is at some distance from it. The behaviour of the two ends of the body is mirror symmetric. The motion of the cylinder along the cavity axis and its contact with the end faces of the cavity are absent.

If we consider the dynamics of one of the ends of the body, then we can say that it oscillates with respect to the angle $\phi_b \approx 60°$ with an amplitude of about 15° in the azimuthal direction and about 1 mm in radial direction. As in the previous state, the body continues to make an unsteady rotation around its own axis. At the moment when one of the cylinder ends approaches its extreme lower position, the gap between the body and the cavity wall becomes minimal and the slowing of the body rotation around its axis is observed. A reduction of the body rotation rate occurs twice for one oscillation period of the body. The second slowdown is associated with the approach of the opposite body end to the cavity boundary. The contact of one of the body ends with the moving cavity wall gives a minor acceleration to its rotation. The average rotation rate of the body around its own axis is 2.5 rad/s.

Body suspension. With further increase in the rotation rate of the cavity, the cylinder is suspended in the laboratory reference frame at some distance from the cavity wall (fig. 7). At $\Omega = 12.6$ rad/s the lift force is large enough to repulse the body from the wall. This is due to an asymmetry between the flows around the body on the side of the cavity wall and on the free side. The body is stably suspended in the fluid due to the fact that the forces acting on it (body weight, lift force and viscous friction) counterbalance each other.

In this state, the cylinder performs azimuthal oscillations of small amplitude in the range $\phi_b = (63.2 \pm 0.4)°$ and radial oscillations of amplitude 0.2 mm. Azimuthal and radial oscillations occur synchronously. With an increase in Ω the cylinder is moved upward (the angle ϕ_b increases). The gap d between the body and the cavity boundary gradually increases: $d = 2.1 \pm 0.1$ mm at $\Omega = 12.6$ rad/s (fig. 7(a)) and $d = 3.0 \pm 0.1$ mm at $\Omega = 16.6$ rad/s (fig. 7(b)).

Instability of the suspended state. With the further increase in Ω, the body, being in the "suspended" state, rises higher along the azimuthal coordinate ϕ_b. The stationary suspended state loses stability after reaching the value $\phi_b \approx 90°$. The body begins to oscillate at $\Omega = 16.9$ rad/s, the amplitude of the body oscillations is small. With the further increase in Ω the amplitude of the body oscillations increases, however the angle ϕ_b remains practically unchanged.

For a more detailed description of the body behaviour in this state we choose such value of Ω, at which the body oscillations are significant. At $\Omega = 17.7$ rad/s, the cylinder is fully detached, and its ends alternately approach the cavity boundary. The trajectory of motion of the centre of body end is an ellipse (fig. 8(a), the arrows indicate the direction of motion). Here, d is the gap between the body end and the cavity boundary. The amplitude of the cylinder oscillations in the radial direction is approximately 4 mm, the azimuthal component of the oscillations of the body end is close to 10°. With an increase in the rotation rate of the cavity, the amplitude of the body oscillations increases. The azimuthal amplitudes of body oscillations in two different regimes ("walking" and instability of the suspension) were close; we can assume that the amplitude is determined by the body length.

The change in the azimuthal coordinate of the body ϕ_b and in the gap d occurs with a small phase shift (fig. 8(b), (c)). The cylinder end touches the cavity wall not in phase with the extreme azimuthal displacement, but with a slight delay. In this case, the cylinder practically uniformly rotates about its axis, with an average speed (10.0 ± 0.8) rad/s (fig. 8(d)). Some irregularity of the rotation rate is observed only when the edge of

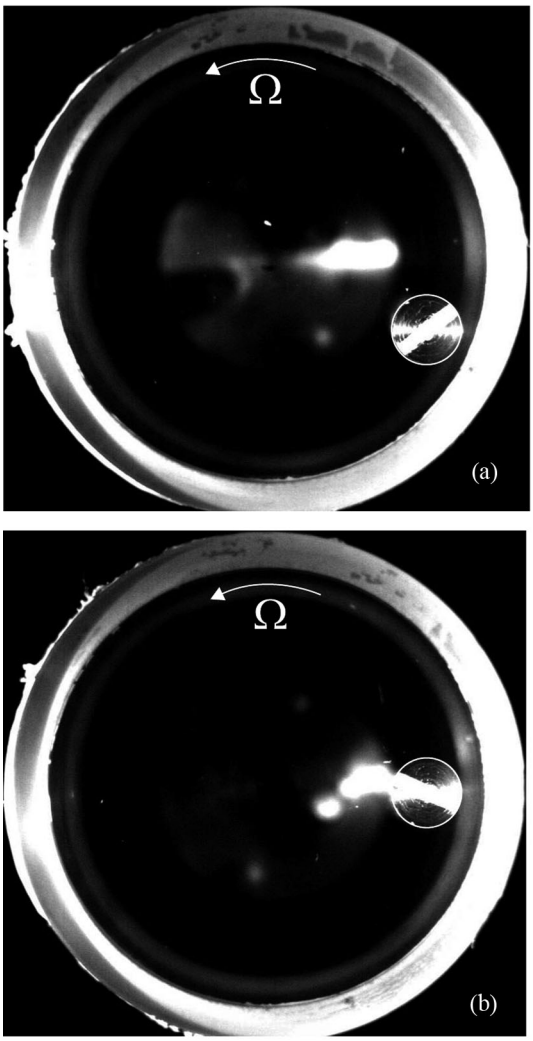

Fig. 7. Suspension of the heavy cylinder near the cavity boundary; $\Omega = 12.6$ rad/s (a) and 16.6 rad/s (b).

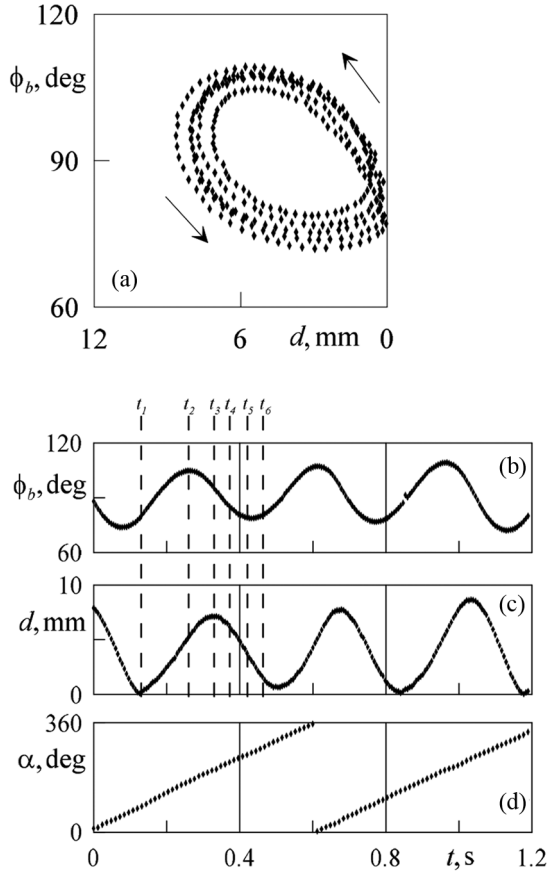

Fig. 8. The change of the gap d between one of the body ends and the cavity boundary, depending on the azimuthal displacement of the end (a). Evolution of the azimuthal coordinate of the body end ϕ_b (b), of the gap between the body end and the cavity wall (c) and of the angle α of the body rotation around its axis (d).

the body contacts the cavity wall, then the rotation speed slightly deviates from the mean value.

Flow structure around the cylinder. Figures 9 and 10 show the average flow structure near the cylinder in the suspension state. This picture is the result of a frame-by-frame processing of a high-speed video recording using the PIV technique. To visualize the flows in the liquid, aluminium powder was added. A light sheet with a width of 5 mm was created with the laser. In the case when the observation was conducted through the front wall of the cavity, the light sheet was oriented perpendicular to the axis of the body at some distance from its end. In the case of side observation, the light sheet, was directed vertically from top to bottom and passed through the centre of the body along its horizontal axis.

Figure 9(a) shows the result of processing a series of body photos in the "suspension" state (side view, light sheet directed along the body axis). The arrows indicate the velocity field of the fluid, the crosses are a mask overlaid on the body to exclude this area from the program calculations. The flow around the body is continuous: on an enlarged fragment of the area near the right end of

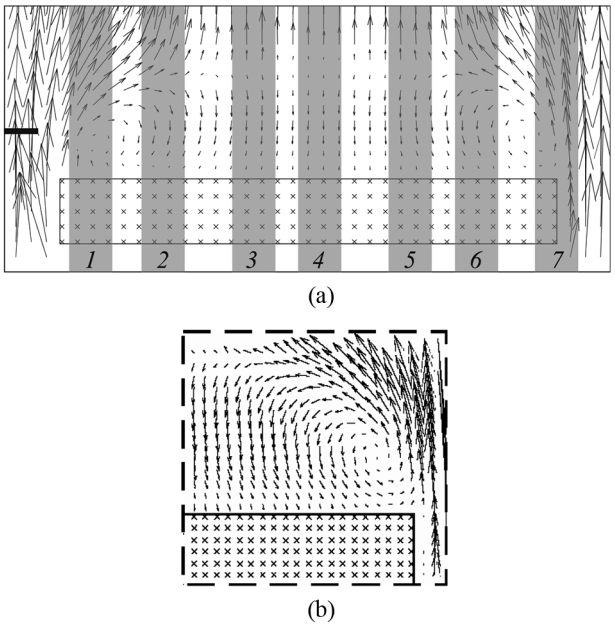

Fig. 9. Flow structure around the suspended cylinder, side view, $\Omega = 11.7$ rad/s.

the body, a stationary vortex is clearly visible (fig. 9(b)). Near the left end of the body there is a mirror-symmetric vortex with the opposite swirl direction. The shaded areas in fig. 9(a), numbered from below, correspond to sections alternately illuminated by the light sheet during video recording through the front end of the cavity (the number 1 denotes the cross-section near the front end of the body, the number 7 denotes the cross-section near the rear).

Fields of fluid velocity directly behind the cylinder in sections 1–7, perpendicular to the axis of rotation, are shown in fig. 10. As is seen in fig. 10(4), the cylinder is suspended in the right part of the cavity. Here, the semicircle indicates the cavity boundary, the circle shows the front end of the body. On the images 1–3 and 5–7, the semicircle indicates the upper half of the body, the vector arrows indicate the fields of fluid velocity. Let us note that near the ends of the body (cross-sections 1 and 7) in the planes perpendicular to its axis, no vortices are observed. Moving a step from the ends towards the centre of the body (cross-sections 2 and 6), one can see a pair of vortices of the opposite swirl direction. In the middle part (3-4-5) the structure of the flow does not change, one of the vortices becomes dominant. It can be expected that if the body length is increased, then practically along its entire length (with the exception of the regions near the ends), the flow structure will be analogous to that shown in fig. 10, 3–5. Comparison of pairs of photos 1–7, 2–6 and 3–5, which are taken at similar distance from the middle of the body, allows us to speak about the symmetry of the flow. The flow near the ends of the cylinder is three dimensional.

Summarizing from velocity vector fields in figs. 9 and 10, the flow structure can be presented in the following way. Along the main part of the body, there is one

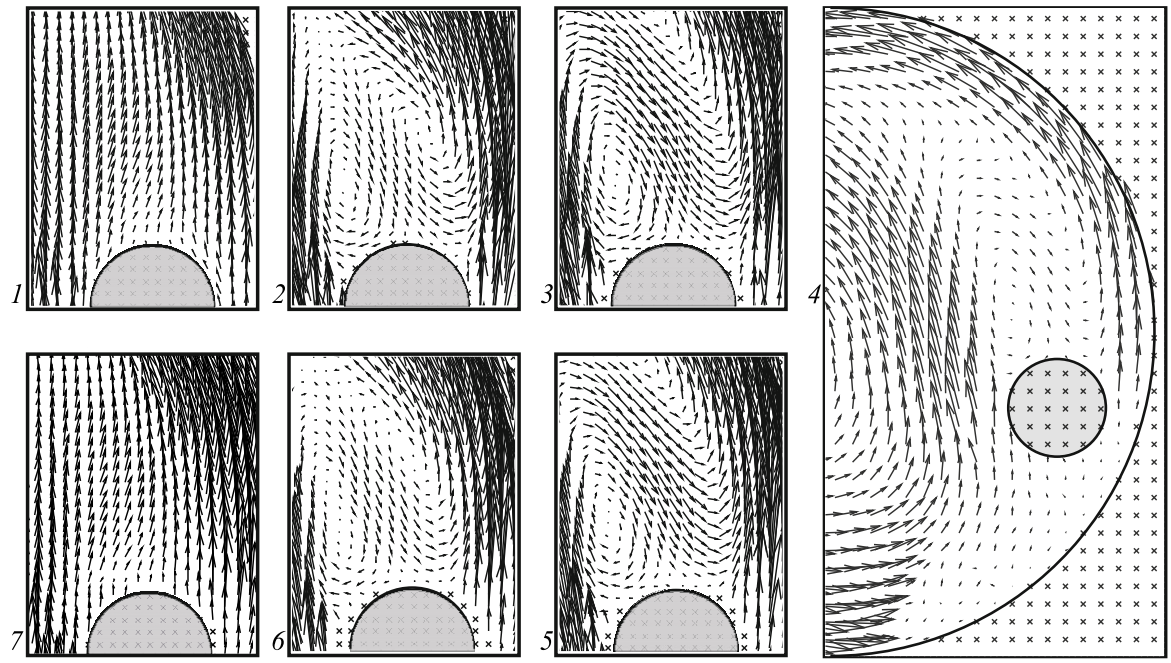

Fig. 10. The fluid velocity field behind the cylinder at different distances from its front ends, $\Omega = 11.7\,\mathrm{rad/s}$.

vortex whose axis is parallel to those of the body and of the cavity (see 1 in fig. 11). The inner structure of vortex 1 does not change with the axial coordinate, so in this region the flow is practically two dimensional. Near the body ends, two symmetric vortices form (see 2 in fig. 11, see fig. 9(b)). The axis of vortex 2 is perpendicular to the body axis. Approximately in the zones of contact between vortices 1 and 2, a symmetric pair of vortices is formed (3 in fig. 11); in the radial projection of this region the flow looks like two counter-rotating vortices (fig. 10, 2, 6). The inner (with respect to the cavity radius) part of vortex 2 is coupled with vortex 1, while its outer part is coupled with vortex 3. Away from the body end-faces, vortices 3 vanish and at the distance of the order of two body diameters in the radial projection one can see only the vortex 1 (5 in fig. 10).

When the body "suspension" loses stability, the main features of the flow structure are pertained: vortices 1, 2 and 3 can be still distinguished. Basically, the flow presented in fig. 11 begins to oscillate. Vortex 1 is transformed: its transversal dimension is not constant along the body length and at different moments its length is also varying, but at all moments it is observed in the middle of the body. Vortices 2 and 3 are changing their location with time, and in the middle of the body length during one oscillation period, one may see either vortex 1 or both vortices 1 and 2. On the body end-faces, vortex shedding is observed.

The structure of the fluid flow in the rotating cavity, when the body is in the unstable suspension mode, is presented in details in fig. 12. Here, we have selected a sequence of photographs reflecting the structure of the flow near the body at the instants noted in fig. 8. The laser sheet is directed perpendicular to the cavity axis and is

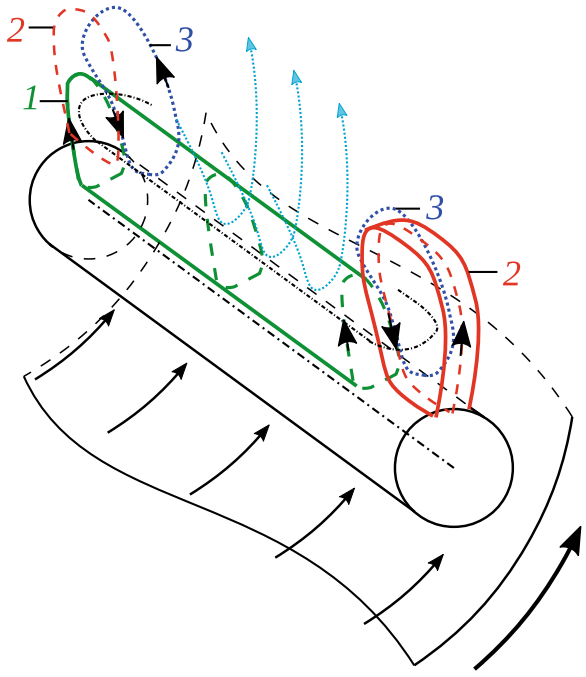

Fig. 11. Scheme of the flow structure in the "suspension" regime of the body motion.

located near the front end of the body (fig. 12(a)) or in the middle of the body (fig. 12(b)). The flow structure is visualized by solid lines constructed from the velocity-field vector data, crosses mark the areas excluded from the calculation. The displacement of the rotation axis of the fluid column leftwards and downwards relative to the cavity axis is visible in the photos. It is clearly seen that when the end of the cylinder moves from bottom to top

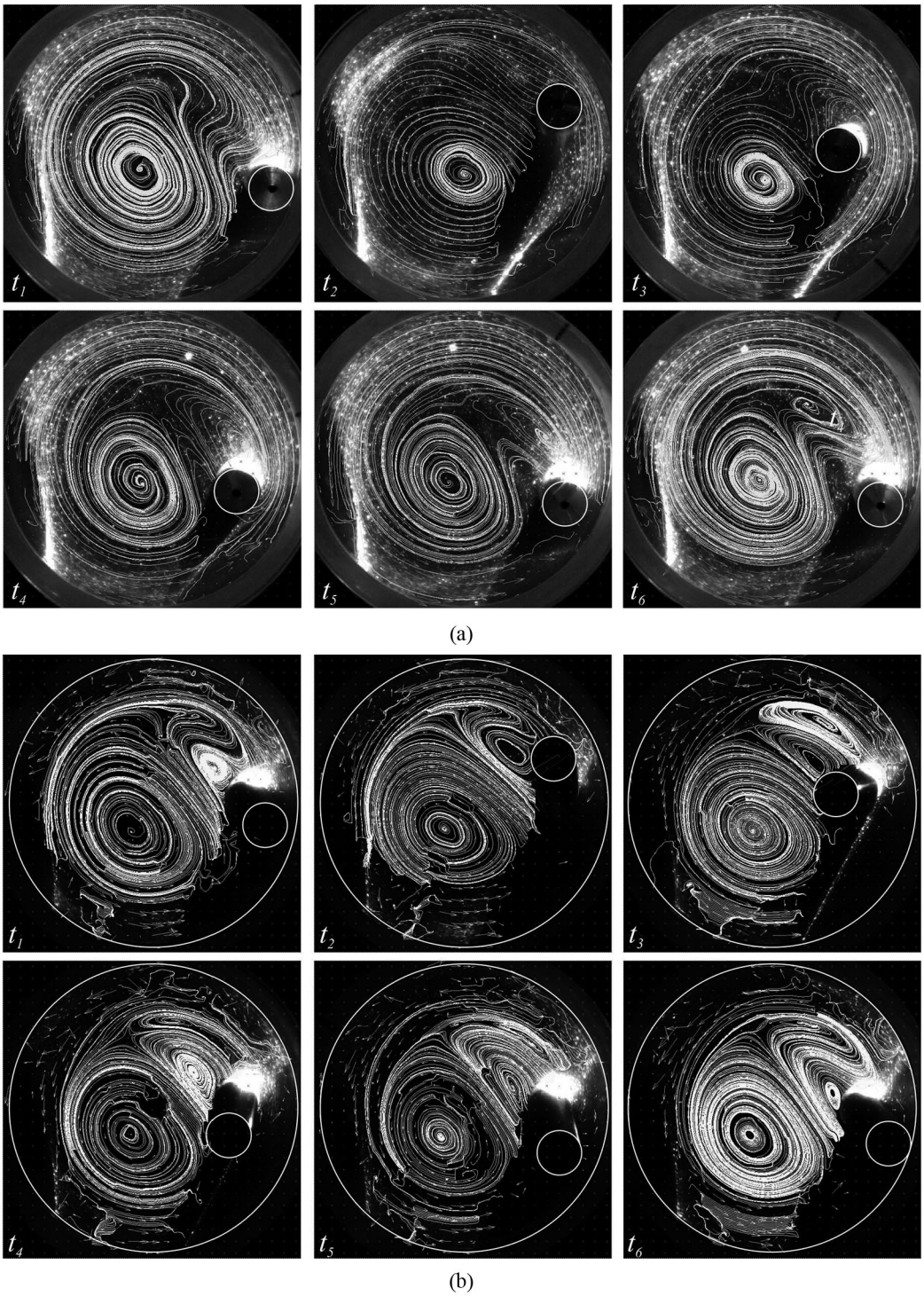

Fig. 12. Visualization of the flow near the front end of the body (a) and the center of the body (b) during one oscillation of the suspended cylinder, $\Omega = 17.7\,\mathrm{rad/s}$.

(moments t_1 and t_2 in fig. 12(a)), there is no vortex formation near it, but when the cylinder moves backward, the flow structure changes: a vortex is formed behind the body which, with its further motion, is detached and carried away by the surrounding fluid flow (moments of time t_3–t_6). In the middle part of the body during the whole period of its oscillations a steady vortex is observed on the inner side of the wake (fig. 12(b)). This vortex is similar to the vortex 1 discovered in the suspension state of the body (fig. 11). When the body's end side moves from top to bottom another vortex of opposite spin is formed. Its dynamics is similar to the dynamics of the vortex near the front body end: at the motion of the front end of the body

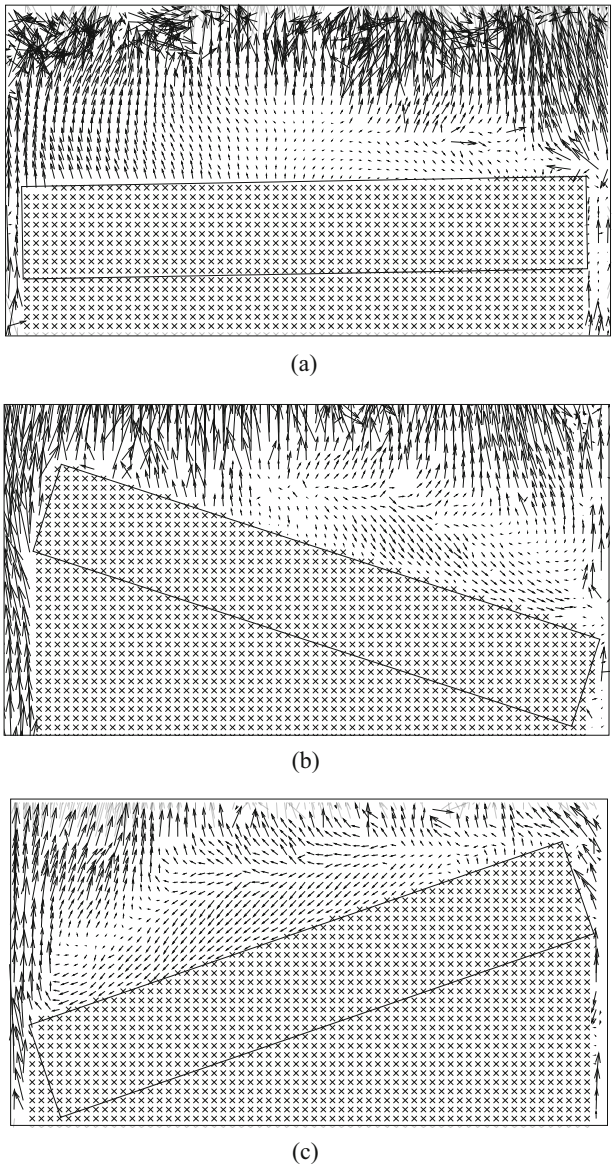

Fig. 13. Visualization of the flow during oscillations of the suspended cylinder, side view, $\Omega = 17.7\,\mathrm{rad/s}$.

from top to bottom it is carried away by the fluid flow and disappears at the body motion from bottom to top.

In this state, the flow around the cylinder is becoming nonstationary and asymmetric, unlike the case of body suspension. Figure 13 shows the velocity fields of the fluid flow in different phases of the cylinder oscillations. When recording images through the side wall of the cavity the laser is installed above the cavity, the direction of the light sheet is set coincident with the average position of the body axis. The arrows indicate the fluid velocity field, the crosses are a mask overlaid on the body and the shadow it creates to exclude this area from the calculations. The rectangle shows the boundaries of the cylinder, here the front end of the body is on the left, the rear end is on the right. At the moment t_1, the cylinder is in a practically horizontal position (fig. 13(a)). In this case, the fluid flow around the front and rear ends of the cylinder is different. In this phase of the body motion the front end is near the cavity wall and the rear end is at some distance from the wall (fig. 12, t_1). As follows from figs. 12 and 13, the flow around the front end is laminar in both the radial (fig. 12) and the longitudinal (fig. 13) cross-sections. Here, the vortex observed in the middle part of the body in fig. 12(b) is visualized by the recurrent fluid motion (the region with smallest vectors in fig. 13(a)). Let us note that the vortex is stretched along the body and most likely represents a roll. The flow around the cylinder in the opposite phases of the oscillations is mirror-symmetric. This is clearly seen in the extreme phases of the body motion (moments t_2 and t_5): the roll shifts from one end to the other during an oscillation (fig. 13(b) and (c)).

Discussion of results

The dynamics of heavy inclusions in rotating cavities with liquid in an external static force field was considered in experimental studies [6,7,13]. Both cylindrical and spherical forms of inclusions are considered in the papers. In [7] authors considered the behaviour of a heavy cylinder with relative density $\rho = 8.01$, relative radius $r/R = 0.2$ in a rotating cylindrical cavity filled with silicone oil of viscosity $\nu = 10\,\mathrm{St}$. It is found that the cylinder is carried away by the wall of the cavity, shifting by some angle, and rotates around its axis. The direction of rotation of the body coincides with the direction of rotation of the cavity, *i.e.* the tangential velocity of the body and the cavity at the point of tangency coincide. With increasing speed of rotation, the angular displacement of the body increases and when the azimuthal position is reached at a value of 10 degrees between the cylinder and the cavity wall a lubrication region formed. In this case, the body slides along the boundary of the cavity, without touching it. In this mode, the velocity of the boundary of the body at the point of contact becomes less than the velocity of the cavity boundary. In this state, the direction of rotation of the body is determined by a chain of cavitation bubbles which formed between the body and the wall. In the case where the bubbles are small and located at a distance from each other, the cylinder rotates in a direction that coincides with the direction of rotation of the cavity. If the size of the bubbles increases up to their contact, the direction of rotation of the cylinder changes to the opposite. The authors explain this effect by the interaction of the body with the flow of a flowing fluid when a continuous chain of cavitation bubbles blocks the lubricant layer. In the present problem, when a cylinder of moderate relative density moves ($\rho = 2.51$) no cavitation bubbles were detected near the boundary. The direction of body rotation in the sliding mode along the wall, as well as in [7], is determined by the direction of rotation of the cavity.

In the work [6], authors pay special attention to the counter-rotating cylinder in a slowly rotating cavity with a liquid ($\nu = 0.01\,\mathrm{St}$). Two states of the body are considered: rolling along the border of the cavity and suspend the body at a distance from the wall. The first state is

similar to the slip mode described in this paper. The body is carried away by the moving wall of the cavity due to viscous interaction, the azimuthal coordinate of the body increases with Ω. At a given rotation rate of the cavity, the body performs azimuthal oscillations of small amplitude about an angle ϕ_b. The maximum angle to which the cylinder rises is $\phi_b \approx 30^\circ$ (in the present work $\phi_b \approx 60^\circ$). As in our work, in this state the direction of rotation of the body is set by friction against the wall of the cavity. Note that after reaching a critical value $\phi_b \approx 30^\circ$ with further increase the body goes into a suspended state, while its azimuthal coordinate increases with Ω. For a cylinder with a relative radius $r/R = 0.13$ the azimuthal position of the body at which the transition to a suspended state occurs is at $\phi_b \approx 10^\circ$, which is several times smaller than in our problem ($r/R = 0.16$, $\phi_b \approx 63.2^\circ$). In this state, despite a significant external force field, the body is in a stable position. We note that, as in our work, here the body performs azimuthal oscillations of small amplitude not exceeding 2°. It is interesting that in [6] the cylinder in the suspended state is rotating in the direction opposite to the direction of rotation of the cavity. The authors explain this by changing the body flow regime and the asymmetric arrangement of stagnation and separation points. In our work, the suspended cylinder rotates about its axis almost uniformly, and in the same direction as the cavity. The average rotation speed of the body is (2.0 ± 0.4) rad/s. It is known that when a body flows over a laminar flow on its solid surface, a boundary layer is formed, the thickness of which is determined by expression $\delta \sim 2r/\sqrt{\mathrm{Re}}$ [14]. The distance to which the cylinder moves away from the wall is of the same order of magnitude as the thickness of the boundary layer $\delta \sim \sqrt{2r\nu/\Omega R} \approx 1\,\mathrm{mm}$. This indicates that the direction of rotation of the body in the suspended state is determined by the viscous interaction with the cavity boundary, due to which the side of the body lower to the wall is entrained in the direction of cavity rotation.

In the work [6] it is noted that the presence of the cylinder in the cavity influences the velocity profile: the latter becomes non-linear, moreover the velocity value decreases compared with the solid-body rotation. In the present work, the decrease of the velocity is discovered too, but its profile remains practically linear (fig. 14). Here V_f is the velocity of the incoming flow, a is the distance between the cavity axis and a fluid element measured along the cavity radius. The value $a = 0.03\,\mathrm{m}$ corresponds to the cavity wall. The angular distance between the body centre and the radial section on which the velocity was measured is about 60 degrees, as well as in [6]. At this distance, the flow does not feel the presence of the body in the cavity: it is rather uniform, while at a shorter distance the flow becomes diverted. On the graph, the solid line shows the law of the solid-body rotation, the pluses show the experimental values of the liquid velocity in the cross-section 1 in fig. 9, the triangles show the velocity in the cross-section 4. It is seen that the experimental velocity is smaller than that of solid-body rotation, like in the work [6]. However in contrast to [6], the velocity profile is linear. Let us note that in the present work the Reynolds

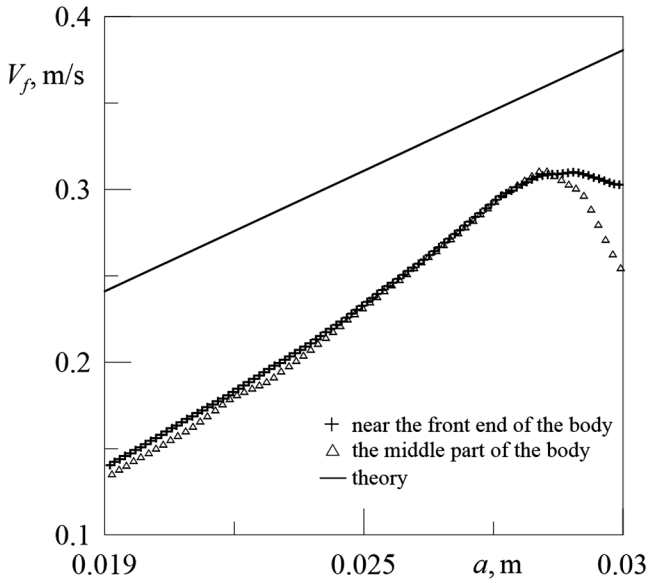

Fig. 14. The profile of the incoming fluid velocity *versus* the radial distance.

number is of the order $\mathrm{Re} \sim 10$–10^2, which is much less than it was in [6], $2500 < \mathrm{Re} < 25000$. Presumably, in the present work the velocity profile is close to linear due to a higher viscosity (smaller Re). The studied profile retains its view with the displacement along the cylinder (fig. 14). A certain decrease in the velocity value near the cavity wall can be associated with some processes in the boundary layer, whose thickness calculated from V_f $\delta = 1.2\,\mathrm{mm}$ is comparable with the region of reduced velocity.

The profile of the incoming fluid velocity allows to calculate the dimensionless lift C_L and drag C_D coefficients from the equations obtained in [6]:

$$C_D = \frac{g\pi r(\rho - 1)\sin\phi_b}{V_f^2},$$

$$C_L = \frac{\pi r(2V_f^2 + g(R - r)(\rho - 1)\cos\phi_b)}{V_f^2(R - r)}.$$

In our work, the coefficients take the values $C_L \approx 2.5$ and $C_D \approx 3.6$. According to the dependence of the coefficient C_D on the Reynolds number given in [6], with a decrease in Re the drag coefficient increases and the minimum value $\mathrm{Re} = 2493 \pm 132$ corresponds to the value $C_D = 1.74 \pm 0.08$. In our work $\mathrm{Re} = 38.1$ corresponds to $C_D \approx 3.6$. The extrapolation of the results presented in [6] gives a qualitative agreement with the present findings. In the case of the lift coefficient, the comparison with the results of [6] is impossible because the dependence of C_L on Re is not given.

Comparing the present results to experimental [15] and numerical [10] results on the flow around a rotating cylinder in the non-rotating fluid, one may notice that the position of vortex 1 (fig. 10, 4 and fig. 11) is in qualitative agreement with these works and may be attributed to the effect of body rotation relative to the fluid. The vortex behind the body is shifted in the direction of its rotation

and is limited on the other side by the laminar flow around the body. Near the body end-faces, vortices 2 bring some returning flow directed towards the body, which cannot be entirely consumed by vortex 1 and contributes to the formation of vortices 3. The latter quickly disappear away from the ends.

In [6], it is noted that in the supercritical ("suspended") regime, with an increase in the cavity rotation speed, the body moves upward along the azimuthal coordinate and, at a threshold value of Ω, loses its stability. In [6], they described the instability of the cylinder as "wiggling", and we assume that they observed the instability studied in the present paper. The loss of stability of the suspended state of the body, as a result of which the body begins to periodically approach the cavity boundary, can be associated with a change in the body flow regime. As can be seen in fig. 12, when the body moves toward the flow, the flow is separated. Note that in this state the body continues to rotate uniformly around its axis. With a further increase in Ω, the oscillation amplitude of the body end-faces increases until they come in contact with the cavity boundary.

Looking at the body trajectory in fig. 8(a), an analogy can be drawn with the dynamics of a spherical body in the rotating fluid. The instability of the suspension of a spherical body in a rotating cavity was observed in [13]. The suspension of the sphere occured at the value $\phi_b \approx 90°$. With a further increase in Ω the sphere, remaining on average near to $\phi_b \approx 90°$, began to perform an orbital motion. The radius of the orbital motion increased with the rotation rate of the cavity.

Conclusions

The dynamics of a heavy cylindrical body in a uniformly rotating cavity with liquid is experimentally studied. It is found that an external static (gravity) field directed perpendicular to the axis of rotation affects the body behaviour. Its dynamics is controlled by two parameters: the ratio between the gravity and centrifugal accelerations Γ and the Reynolds number. There are five motion regimes. Three are steady —sliding, suspension and centrifuged motion. Two are unsteady —"walking" and precession, and they are transitions between the steady regimes. The change in the behaviour of the body is related to the change in the rotation speed of the cavity, which determines the balance between the drag and lift forces acting on the body. It is shown that in each of the regimes the body rotates about its axis, due to a viscous interaction with the cavity wall. The time-dependent dynamics of the body is investigated, the trajectories of its motion are reconstructed, and the flow structures near the cylinder are studied. It is shown that in the centrifuged state the body has no effect on the flow structure: the rotation axis of the fluid column coincides with the cavity axis. Meanwhile in other regimes, the fluid column axis is shifted away from the cylindrical body. A common feature for all motion regimes is the presence of a convective roll extended parallel to the body. In the case of the steady body's suspension, the transversal size of the roll is of the same order of magnitude as the body diameter, while in the cases of "walking" and precession the roll is noticeably larger than the cylinder. Generally, the flow structure is three dimensional, especially on the body ends. The role of the body end-faces proved to be important. It is found that the instability of the "suspension" is related to a change in the regime of flow past the body and is accompanied by a periodic vortex shedding from its ends. It is interesting that the flow is laminar in all experiments, the maximum Reynolds number being $\mathrm{Re} \approx 120$. This result agrees with [9], where the transition to turbulence is predicted for $\mathrm{Re} > 200$.

The work was done with the support from the Russian Foundation for Basic Research (grant 16-31-00201) and is an evolution of the research started in the frame of the Russian Science Foundation project 14-11-00476.

Author contribution statement

Olga Vlasova and Nikolai Kozlov developed and built the experimental setup, implemented the measurement and processing methods, performed the analysis of results and wrote the article.

References

1. V.L. Sennitskii, J. Appl. Mech. Tech. Phys. **26**, 620 (1985).
2. V.G. Kozlov, Europhys. Lett. **36**, 651 (1996).
3. A.A. Ivanova *et al.*, J. Appl. Mech. Tech. Phys. **55**, 773 (2014).
4. H.P. Greenspan, *The Theory of Rotating Fluids* (CUP Archive, 1968).
5. G.B. Jeffery, Proc. R. Soc. London, Ser. A **101**, 169 (1922).
6. C. Sun *et al.*, J. Fluid Mech. **664**, 150 (2010).
7. J.R.T. Seddon, T. Mullin, Phys. Fluids. **18**, 041703 (2006).
8. E.A. Van Nierop *et al.*, J. Fluid Mech. **571**, 439 (2007).
9. B.M. Sumer, J. Fredsoe, *Hydrodynamics Around Cylindrical Structures* (World Scientific, 2006).
10. S. Mittal, B. Kumar, J. Fluid Mech. **476**, 303 (2003).
11. H.M. Badr, S.C.R. Dennis, J. Fluid Mech. **158**, 447 (1985).
12. N.V. Kozlov, O.A. Vlasova, Fluid Dyn. Res. **48**, 055503 (2016).
13. Y. Tagawa *et al.*, Phys. Fluids **25**, 063302 (2012).
14. H. Schlichting, *Boundary-Layer Theory* (New York, McGraw-Hill, 1979).
15. H.M. Badr *et al.*, J. Fluid Mech. **220**, 459 (1990).